

Published in final edited form as:

J Neurosci. 2012 January 25; 32(4): 1253–1260. doi:10.1523/JNEUROSCI.4652-11.2012.

Calcium Binding by Synaptotagmin's C₂A Domain is an Essential Element of the Electrostatic Switch that Triggers Synchronous Synaptic Transmission

Amelia R. Striegel^{1,a}, Laurie M. Biela^{1,a}, Chantell S. Evans², Zhao Wang², Jillian B. Delehoy¹, R. Bryan Sutton³, Edwin R. Chapman², and Noreen E. Reist^{1,*}

¹Department of Biomedical Sciences, Program in Molecular, Cellular, and Integrative Neuroscience, Colorado State University, Fort Collins, Colorado, USA 80523

²Department of Neuroscience, University of Wisconsin, Madison, Wisconsin, USA 53706

³Department of Cell Physiology and Molecular Biophysics, Texas Tech University Health Sciences Center, Lubbock, Texas, USA 79409

Abstract

Synaptotagmin is the major calcium sensor for fast synaptic transmission which requires the synchronous fusion of synaptic vesicles. Synaptotagmin contains two calcium binding domains: C₂A and C₂B. Mutation of a positively charged residue (R233Q in rat) showed that Ca²⁺-dependent interactions between the C₂A domain and membranes play a role in the electrostatic switch that initiates fusion. Surprisingly, aspartate to asparagine mutations in C₂A that inhibit Ca²⁺ binding support efficient synaptic transmission, suggesting that Ca²⁺ binding by C₂A is not required for triggering synchronous fusion. Based on a structural analysis, we generated a novel mutation of a single Ca²⁺-binding residue in C₂A (D229E in *Drosophila*) that inhibited Ca²⁺ binding, but *maintained* the negative charge of the pocket. This C₂A aspartate to glutamate mutation resulted in ~80% decrease in synchronous transmitter release and a decrease in the apparent Ca²⁺ affinity of release. Previous aspartate to asparagine mutations in C₂A partially mimicked Ca²⁺ binding by decreasing the negative charge of the pocket. We now show that the major function of Ca²⁺ binding to C₂A is to neutralize the negative charge of the pocket, thereby unleashing the fusion-stimulating activity of synaptotagmin. Our results demonstrate that Ca²⁺ binding by C₂A is a critical component of the electrostatic switch that triggers synchronous fusion. Thus, Ca²⁺ binding by C₂B is necessary and sufficient to regulate the precise timing required for coupling vesicle fusion to Ca²⁺ influx, but Ca²⁺ binding by both C₂ domains is required to flip the electrostatic switch that triggers efficient synchronous synaptic transmission.

Keywords

C₂A; synchronous release; Ca²⁺ sensor; electrostatic switch

Introduction

Synaptic transmission occurs when Ca²⁺ entry into an active nerve terminal triggers the fast, synchronous fusion of synaptic vesicles with the presynaptic membrane. Shortly after the identification of its two C₂ domains, synaptotagmin was postulated to be the Ca²⁺ sensor

*Corresponding author: Dr. Noreen E. Reist, Dept of Biomedical Sciences, Colorado State University, Fort Collins, CO 80523, Phone: 970-491-5882, FAX: 970-491-7907, Noreen.Reist@Colostate.edu.

^aEqually contributing authors

Fly Lines

Expression of the transgene was localized to the nervous system using elavGal4 to drive pan neuronal expression of the UAS-*syt* transgenes (Brand and Perrimon, 1993; Yao and White, 1994). The *syt^{null}* mutation used was *syt^{AD4}* (DiAntonio et al., 1993). Standard genetic techniques were used to cross the transgenes into the *syt^{null}* background in order to express the transgene in the absence of endogenous synaptotagmin 1 (Loewen et al., 2006a). No gender selection was employed, thus a mix of male and female larvae were used in all experiments. Experimental flies were: *yw; syt^{null}elavGAL4/syt^{null}; P[UAS *syt^{A-D229E}]/+* (*P[syt^{A-D2E}]*, transgenic mutant) and *yw; syt^{null}elavGAL4/syt^{null}; P[UAS *syt^{WT}]/+* (*P[syt^{WT}]*, transgenic control).**

Sequence Alignments

A ClustalW2 sequence alignment was performed on the C₂A domain of the following Ca²⁺-binding synaptotagmin isoforms: *syt 1* from *Drosophila melanogaster* (NP_523460.2), *Apis mellifera* (NP_001139207.1), *Manduca sexta* (AAK01129.1), *Loligo pealei* (BAA09866.1), *Caenorhabditis elegans* (NP_495394.3), *Gallus gallus* (NP_990502.1), *Mus musculus* (NP_033332.1), *Rattus norvegicus* (NP_001028852.2), and *Homo sapiens syt 1* (NP_001129277.1), *syt 2* (NP_001129976.1), *syt 3* (NP_001153801.1), *syt 5* (NP_003171.2), *syt 6* (NP_995320.1), *syt 7* (NP_004191.2), *syt 9* (NP_445776.1), and *syt 10* (NP_945343.1).

Molecular Modeling

The D2E mutation in Fig 1C was modeled using the mutagenesis plugin in PyMOL (The PyMOL Molecular Graphics System, Version 1.3, Schrödinger, LLC). Asp-178, from the high resolution rat synaptotagmin 1 C₂A X-ray structure (1RSY), was changed to a glutamate. The rotamer with the fewest number of collisions was selected for the figure.

Electrophysiology

EJPs and mEJPs were recorded using standard techniques (Reist et al., 1998; Paddock et al., 2011) from L3 muscle fiber 6 of abdominal segments 3 and 4 in HL3 saline containing 70 mM NaCl, 5 mM KCl, 20 mM MgCl₂, 10 mM NaHCO₃, 5 mM Trehalose, 115 mM sucrose, 5 mM HEPES, pH 7.2, and 1.5 mM CaCl₂ unless otherwise indicated. Dissections were performed in Ca²⁺-free HL3 saline. Fibers were impaled with a 10–40 MΩ recording electrode containing 3 parts 2 M potassium citrate to 1 part 3 M potassium chloride. The resting membrane potential of each fiber was maintained at –55 mV by passing a bias current. To evoke EJPs, segmental nerves were stimulated with a suction electrode filled with 1.5 mM Ca²⁺ HL3. The Ca²⁺ dependence curve was generated by averaging 10 EJPs recorded at 0.5 Hz from fibers bathed in HL3 containing Ca²⁺ concentrations ranging from 0.6 to 5.0 mM. Recordings in multiple Ca²⁺ concentrations were made from each muscle fiber. 10–13 fibers were recorded at each Ca²⁺ concentration in each genotype with the exception of 1.5 mM Ca²⁺. 28–34 fibers were recorded at 1.5 mM Ca²⁺ since most recording sessions included this concentration. All events were collected using an AxoClamp 2B (Molecular Devices) and digitized using a MacLab4s A/D converter (ADInstruments). The Ca²⁺-dependence data were fit with the Hill equation using Kaleidagraph software. The Ca²⁺ cooperativity coefficient was estimated from the slope of a double-log plot of EJP amplitude versus Ca²⁺ concentration. EJPs were recorded in Scope software and mEJPs were recorded in Chart Software (ADInstruments).

Immunoblotting and immunohistochemistry

Western analysis was used to determine levels of transgene expression. The central nervous systems of individual third instar larvae were loaded 1 CNS/lane and blots were probed with

an anti-synaptotagmin antibody [Dsynt-CL1 (Mackler et al., 2002)] and an anti-actin antibody (MAB 1501, Chemicon) using standard techniques (Loewen et al., 2001). Actin levels were used to normalize for equal protein loading; the synaptotagmin:actin signal ratio was determined for each lane, then normalized to the mean synaptotagmin:actin ratio of the *P[syt^{WT}]* lanes on each blot to allow comparison of signal between multiple blots. Transgenic synaptotagmin was localized by immunolabeling third instar larvae with Dsynt-CL1 using standard techniques (Mackler and Reist, 2001). Neuromuscular junctions were visualized on a Zeiss Axioplan 2 upright digital imaging microscope.

CD spectroscopy

CD spectra were measured with an AVIV stop flow Circular Dichroism spectropolarimeter at 192 to 260 nm using a 1 mm path-length cell. Samples containing 0.2 mg/ml of either wild type or mutant C₂A domains were assayed at 22 °C. For corrections of baseline noise, the signal from a blank run of buffer (50mM sodium phosphate) was subtracted from all the experimental spectra.

Isothermal titration calorimetry

Isothermal titration calorimetry (ITC) data was generated using a GE Healthcare MicroCal iTC₂₀₀ which can in principle detect dissociation constants from 10 mM to 1 nM. Wild type and mutant C₂A domains were dialyzed overnight in ITC buffer (50 mM HEPES, pH 7.4, 200 mM NaCl, and 10% glycerol). ITC buffer was further used to make calcium chloride stock and protein dilutions. Prior to each experiment, samples were degassed and cooled to experimental temperature. Heat of binding was measured from thirty 1.1 µl injections of calcium chloride into sample cells containing 1.6 mg/ml of proteins of interest at 15° C. Baseline corrections, for heat of dilution, were made by subtracting the signal of calcium chloride injections into buffer from all experimental traces. Data was analyzed using GE Healthcare MicroCal iTC₂₀₀ Origin data software package.

Statistical Analyses

A Student *t*-test was used to determine whether any statistically significant differences existed between the two independent *P[syt^{A-D2E}]* lines (line 3 and line 5). One-way ANOVA and Tukey range tests were used for statistical comparisons of *P[syt^{WT}]* and the two *P[syt^{A-D2E}]* lines.

Results

Sequence and structural analyses of C₂A

C₂ domains are a common functional motif found in multiple proteins. Although not all C₂ domains are regulated by Ca²⁺, many C₂ domains mediate a Ca²⁺-dependent translocation of the protein to membranes (Nalefski and Falke, 1996; Cho and Stahelin, 2006). In these proteins, Ca²⁺ is coordinated by five negatively-charged residues located in loops 1 and 3 of the C₂ domain beta-sandwich structure [e.g., see Fig. 1A,B: D1–5 (Sutton et al., 1995; Nalefski and Falke, 1996; Ubach et al., 1998)]. Both aspartate and glutamate residues are utilized in the Ca²⁺-binding motifs of diverse C₂ domains (Nalefski and Falke, 1996). To assess whether Ca²⁺ binding by C₂A could be supported by either aspartate or glutamate residues, we compared the sequence of C₂A domains of synaptotagmin isoforms that bind Ca²⁺. A sequence alignment revealed that glutamate is excluded from these key positions. In the C₂A Ca²⁺-binding motifs of synaptotagmin 1 from many species, as well as of all of the human synaptotagmin isoforms that bind Ca²⁺, all 5 aspartate residues are 100% conserved (Fig. 1A) suggesting that glutamate residues in these positions would not provide full function.

Examination of the crystal structure of rat syt 1 C₂A demonstrates that the deepest parts of this Ca²⁺-binding pocket are spatially quite restricted (Sutton et al., 1995). Glutamate, like aspartate, is negatively charged, but glutamate possesses a significantly larger molecular volume [91 Å³ for Asp vs. 109 Å³ for Glu (Creighton, 1994)]. Coupled with the exclusion of glutamate from C₂A Ca²⁺-binding motifs, this observation suggested that a D→E mutation may impair Ca²⁺ binding. In the crystal structure of rat syt 1 C₂A, both aspartate residue 178 (Fig. 1A,B: D2) and aspartate residue 230 (Fig. 1A,B: D3) are well ordered and located deep in the Ca²⁺-binding pocket (Sutton et al., 1995). To assess whether a D→E mutation in either of these locations may occlude the Ca²⁺-binding pocket, we modeled the C₂A^{D2E} and C₂A^{D3E} mutations *in silico*. Results suggested that the C₂A^{D2E} mutation might occlude Ca²⁺-binding site 1 (Fig. 1C: Ca1 site). If true, this novel mutation would directly assess the importance of the electrostatic repulsion provided by C₂A in inhibiting vesicle fusion since it would inhibit Ca²⁺ binding without reducing the negative charge of the pocket (Fig. 1C: red regions).

The syt^{A-D2E} mutation inhibits Ca²⁺ binding to C₂A

To directly measure Ca²⁺ binding to the C₂A domain of *Drosophila* synaptotagmin 1, we utilized isothermal titration calorimetry (ITC). The titration data indicate three Ca²⁺-binding sites in *Drosophila* C₂A (Fig. 2A, Table 1). The intrinsic Ca²⁺ affinities of the three sites measured by ITC (Table 1, K_{DS} = 20.7 ± 3.9 μM, 83.4 ± 19 μM, and 766 ± 302 μM, respectively) were in the same range, though the K_{DS} were somewhat lower, than those in previous reports on murine synaptotagmin using NMR (Shao et al., 1996; Ubach et al., 1998). As predicted, Fig. 2A demonstrates that the C₂A^{D2E} mutation inhibited Ca²⁺ binding by the C₂A domain. We assessed protein folding by circular dichroism (CD) spectroscopy to exclude misfolding of the mutant C₂A domain. As shown in Fig. 2B, the C₂A^{D2E} mutation does not alter the CD spectrum as compared to wild-type C₂A. Thus, our novel C₂A mutation is correctly folded and largely inhibits Ca²⁺ binding by the C₂A domain. D2 only directly coordinates the first Ca²⁺ site (Fig. 1B: D2---Ca1). If the C₂A^{D2E} mutation does in fact remove all Ca²⁺ binding, this would support a model in which Ca²⁺ binding to site 1 is requisite for Ca²⁺ binding to sites 2 and 3.

C₂A Ca²⁺-binding mutant inhibits synchronous transmitter release *in vivo*

To determine the importance of electrostatic repulsion by the C₂A domain for synchronous synaptic transmission at an intact synapse, we examined evoked transmitter release at *Drosophila* neuromuscular junctions expressing our mutant transgenic synaptotagmin protein (syt^{A-D2E}) in the absence of any wild-type synaptotagmin 1. To indicate its transgenic origin, we will refer to the mutant as *P[syt^{A-D2E}]* and the transgenic controls as *P[syt^{WT}]*. We found that the syt^{A-D2E} Ca²⁺-binding motif mutation, which maintains the negative charge of the C₂A pocket, decreased synchronous evoked release by >80% (Fig. 3A,B). The amplitude of the excitatory junction potential (EJP) in *P[syt^{A-D2E}]* was 5.16 ± 0.96 mV (line 3, n=11) or 2.84 ± 0.41 mV (line 2, n=8) compared with 34.19 ± 3.97 (n=8) in *P[syt^{WT}]* controls [Fig. 3A (line 3 shown) and Fig. 3B, p<<0.001]. There was no significant difference between the independent mutant lines (p>0.07) demonstrating that the decrease in evoked release is not due to the insertion sites of the transgene, but rather is a direct result of the mutation.

Since analogous aspartate to asparagine mutations in C₂A, which also inhibit Ca²⁺ binding but partially neutralize the negative charge of the pocket, did *not* significantly impair synchronous evoked release at this same synapse (Robinson et al., 2002; Yoshihara et al., 2010), or at cultured excitatory synapses (Fernandez-Chacon et al., 2002; Stevens and Sullivan, 2003), our findings demonstrate that the key function of Ca²⁺ binding to the C₂A domain is to neutralize the negative charge of the C₂A Ca²⁺-binding pocket. Thus, Ca²⁺

binding to the C₂B domain is necessary and sufficient for *synchronizing* synaptic vesicle fusion to Ca²⁺ influx (Mackler et al., 2002; Robinson et al., 2002), as seen by the low level of fast, synchronous, evoked release that remains in our *P[syt^{A-D2E}]* mutants (Fig. 3A,B). But it is *not sufficient* to efficiently trigger the electrostatic switch. Efficient, synchronous release requires Ca²⁺ binding to the C₂A and C₂B domains to neutralize both negatively-charged Ca²⁺-binding pockets and flip the electrostatic switch resulting in fast, synchronous vesicle fusion.

C₂A mutant does not impact spontaneous transmitter release

The C₂A Ca²⁺-binding motif mutation had no significant effect on either the amplitude or frequency of spontaneous transmitter release. The amplitude of miniature excitatory junction potentials (mEJPs) in *P[syt^{A-D2E}]* was 0.69 ± 0.03 mV (line 3, n=12) or 0.68 ± 0.03 mV (line 2, n=12) compared to 0.70 ± 0.02 mV (n=12) in *P[syt^{WT}]* (Fig. 3C, $p > 0.7$). The constant mEJP amplitude demonstrates that synaptic vesicle filling and the postsynaptic response to neurotransmitter are unimpaired. The frequency of mEJPs in the C₂A mutants was also not significantly different at 3.71 ± 0.52 Hz (line 3), or 4.45 ± 0.37 Hz (line 2) in *P[syt^{A-D2E}]* compared to 3.19 ± 0.48 Hz in *P[syt^{WT}]* controls (Fig. 3D, $p > 0.15$). Since this C₂A Ca²⁺-binding motif mutation results in a large decrease in evoked release (Fig. 3A,B), yet does *not* affect the rate of spontaneous release (Fig. 3A,D), the increase in spontaneous release seen in other synaptotagmin point mutants (Mackler and Reist, 2001; Mackler et al., 2002; Paddock et al., 2008) cannot be explained as an indirect developmental artifact resulting from the decrease in evoked release. Rather, our findings support the hypothesis that synaptotagmin plays a direct role in regulating the rate of spontaneous release (Broadie et al., 1994; Morimoto et al., 1995; Mace et al., 2009) and that the negative charge of the C₂A Ca²⁺-binding pocket plays a key role in this process. Indeed, when Ca²⁺ binding is inhibited by D→N mutations of the C₂A Ca²⁺-binding pocket, the rate of spontaneous release is increased 6-fold (Yoshihara et al., 2010). This dramatic difference in the effect on spontaneous fusion frequency between D→N mutations and our D→E mutation demonstrates that the electrostatic repulsion created by the negative charge in the C₂A Ca²⁺-binding pocket *must* be neutralized to enhance any fusion.

C₂A mutants decrease apparent Ca²⁺ affinity of release

To assess whether the decrease in evoked release resulted from changes in either the apparent Ca²⁺ affinity or cooperativity of release, we measured EJP amplitudes in extracellular Ca²⁺ concentrations ranging from 0.6 mM to 5 mM. *P[syt^{A-D2E}]* had a significantly reduced evoked response compared to the control at every extracellular Ca²⁺ concentration (Fig. 3E). To facilitate comparison, the data were plotted as a percentage of the maximal response (Fig. 3F). The apparent Ca²⁺ affinity of release *in vivo* was decreased in the *P[syt^{A-D2E}]* mutants; 45% more Ca²⁺ was required to trigger a half maximal response ($EC_{50} = 1.92 \pm 0.26$ mM) compared to *P[syt^{WT}]* controls ($EC_{50} = 1.33 \pm 0.18$ mM). By plotting the mean EJP amplitude against the extracellular Ca²⁺ concentration at non-saturating levels on a double log plot (Fig. 3G), we found that the Ca²⁺ cooperativity of release was not affected by the *syt^{A-D2E}* mutation [$n = 2.52$ for *P[syt^{A-D2E}]* and $n = 2.69$ for *P[syt^{WT}]*], similar to previously reported values at wild type neuromuscular junctions in *Drosophila* (Stewart et al., 2000; Okamoto et al., 2005). The shift in the Ca²⁺ affinity of release with no effect on the cooperativity of release is consistent with the stochastic model of cooperativity (Dodge and Rahamimoff, 1967; Stewart et al., 2000; Fernandez-Chacon et al., 2001; Mackler et al., 2002). However some synaptotagmin mutations alter the cooperativity of release which would favor the stoichiometric model (Dodge and Rahamimoff, 1967; Yoshihara and Littleton, 2002; Tamura et al., 2007). Further work will be necessary to discriminate between these models. Regardless, the decrease in the apparent Ca²⁺ affinity of evoked release is consistent with the finding that the *syt^{A-D2E}* mutation

specifically inhibits Ca^{2+} binding by the C_2A domain and demonstrates that Ca^{2+} binding by C_2A is essential for fast, synchronous synaptic transmission.

Transgene expression and distribution are unaffected

Since a decrease in synchronous evoked release could also result from protein misexpression, we assessed transgenic synaptotagmin expression levels in each transgenic line. Western blot analysis of third instar larval central nervous systems with an anti-synaptotagmin antibody demonstrated that the C_2A Ca^{2+} -binding motif mutant lines expressed similar levels of transgenic synaptotagmin as the transgenic control (Fig. 4A,B). In addition, the mutant synaptotagmin was appropriately localized to the neuromuscular junction (Fig. 4C). Therefore, the deficits in evoked release are not due to insufficient protein expression or protein mislocalization.

Discussion

Our results now clearly demonstrate that Ca^{2+} binding by the C_2A domain is a key functional component of the electrostatic switch that triggers synchronous synaptic vesicle fusion. A comparison of multiple C_2A Ca^{2+} -binding mutants reveals that the key function of Ca^{2+} binding by C_2A is to neutralize the negative charge of this pocket. Our $\text{D}\rightarrow\text{E}$ mutant inhibits Ca^{2+} binding but maintains the negative charge of the C_2A pocket. $\text{D}\rightarrow\text{N}$ mutants also inhibit Ca^{2+} binding, but they decrease the negative charge of the C_2A pocket. Neutralization of the C_2A pocket results in a dramatic increase in the fusion-stimulating activity of synaptotagmin.

Our C_2A $\text{D}\rightarrow\text{E}$ mutant inhibits Ca^{2+} binding but maintains the negative charge of the C_2A pocket. With the repulsive force of the C_2A domain intact, both synchronous release and the apparent Ca^{2+} affinity of release were decreased. In C_2A $\text{D}\rightarrow\text{N}$ mutants, synchronous transmitter release proceeds efficiently with Ca^{2+} binding to C_2B providing the synchronization to Ca^{2+} influx (Fernandez-Chacon et al., 2002; Robinson et al., 2002; Yoshihara et al., 2010). Indeed, C_2A $\text{D}\rightarrow\text{N}$ mutants that include D4N enhanced synchronous fusion as shown by an *increase* in the apparent Ca^{2+} affinity of release (Stevens and Sullivan, 2003; Pang et al., 2006; Yoshihara et al., 2010). The major difference between these mutants is the charge of the Ca^{2+} -binding pocket. Thus, the electrostatic repulsion provided by the C_2A domain must be neutralized, by either Ca^{2+} binding or mutation, to activate synaptotagmin's fusion-stimulating function during synchronous transmitter release. Interestingly, one multiple C_2A mutant ($\text{C}_2\text{A}^{\text{D}2,3,4\text{A}}$) that both inhibits Ca^{2+} binding and neutralizes the negative charge of the pocket decreased synchronous release by ~30% at cultured inhibitory synapses (Shin et al., 2009). Yet similar multiple C_2A $\text{D}\rightarrow\text{N}$ mutations (even the $\text{C}_2\text{A}^{\text{D}1-5\text{N}}$ mutation) do not decrease synchronous release (Stevens and Sullivan, 2003). The effect of these mutations on spontaneous release was not reported. This differential effect may indicate that neutral asparagine (vs. alanine) residues more closely mimic Ca^{2+} -bound aspartates. Regardless of the source of these differences, the finding that our C_2A $\text{D}\rightarrow\text{E}$ mutation inhibits synchronous release by 80% demonstrates that the major mechanism utilized by C_2A to inhibit synaptotagmin's fusogenic activity is electrostatic repulsion.

The effect of mutations on spontaneous vesicle fusion events demonstrates that the negative charge of the C_2A pocket acts as a clamp to inhibit an inherent fusion-stimulating activity of synaptotagmin. Our C_2A $\text{D}\rightarrow\text{E}$ mutation maintains the ability of synaptotagmin to suppress spontaneous release, while C_2A $\text{D}\rightarrow\text{N}$ mutations result in a massive increase in spontaneous vesicle fusion events (Yoshihara et al., 2010). Thus, regardless of the downstream effector interaction(s) that mediate the fusion reaction, the negative charge of the C_2A Ca^{2+} -binding pocket functionally inhibits synaptic vesicle fusion until neutralized.

D→N mutations in both C₂A and C₂B *increase* the rate of spontaneous transmitter release (Mackler et al., 2002; Yoshihara et al., 2010), in effect removing the need for Ca²⁺ to unleash the fusion-stimulating activity of synaptotagmin. So why do these mutations impact synchronous release so differently? C₂B D→N mutants nearly completely block synchronous release (Mackler et al., 2002) while C₂A D→N mutants don't (Fernandez-Chacon et al., 2002; Robinson et al., 2002; Yoshihara et al., 2010). Here we propose a possible mechanism (Fig. 5) that may contribute to this differential action, although additional interactions must also be involved as noted below.

C₂B, by virtue of its Ca²⁺-independent priming interaction with the SNARE complex (Rickman et al., 2004; Loewen et al., 2006b) and being the vesicle distal C₂ domain, would be located *immediately adjacent* to the presynaptic membrane while C₂A is likely further removed. Prior to Ca²⁺ entry, electrostatic repulsion prevents interactions between the C₂ domains and the negatively-charged presynaptic membrane (Fig. 5A,B “-” signs). Ca²⁺ influx initiates the electrostatic switch: an immediate change from electrostatic repulsion (due to the negatively charged residues) to electrostatic attraction of the negatively-charged presynaptic membrane (due to the bound Ca²⁺ and the conserved, positively-charged residue; Fig. 5B,C, blue stick residue, +) which pulls the vesicle toward the presynaptic membrane. Hydrophobic residues on the tip of the C₂ domain (Fig. 5B,C, grey stick residues) can then penetrate the presynaptic membrane, destabilizing it and promoting the fusion reaction by pulling the presynaptic membrane toward the vesicle in a ring around the site of SNARE-mediated fusion (Fig. 5D). Since C₂B is located immediately adjacent to the presynaptic membrane, it would attract and penetrate the membrane first (Bai et al., 2002; Wang et al., 2003; Herrick et al., 2006; Fuson et al., 2007; Martens et al., 2007; Paddock et al., 2008; Hui et al., 2009; Paddock et al., 2011). This action may then pivot the vesicle proximal C₂A domain toward the membrane where it can also then participate in the electrostatic attraction and hydrophobic penetration activities (Fernandez-Chacon et al., 2001; Bai et al., 2002; Wang et al., 2003; Herrick et al., 2006; Paddock et al., 2008; Paddock et al., 2011). When interactions of the C₂B domain with the presynaptic membrane are prevented by mutation, the C₂A domain would not be pivoted into position for interactions with the membrane and synaptic transmission would be blocked (Mackler et al., 2002; Paddock et al., 2011). When Ca²⁺ binding by the C₂A domain is inhibited via D→N mutations, the decreased negative charge of the pocket may partially mimic Ca²⁺ binding (Stevens and Sullivan, 2003) permitting the remaining C₂A lipid-interacting residues to bind and penetrate the presynaptic membrane when C₂B pivots the C₂A domain into position. Thus, these C₂A mutations would result in little to no disruption in evoked release (Fernandez-Chacon et al., 2002; Robinson et al., 2002; Stevens and Sullivan, 2003; Pang et al., 2006). Removal of the C₂A positively-charged residue (Fig. 5B,C: C₂A blue “+” residue) or the hydrophobic residues (Fig. 5B,C: C₂A grey stick residues), on the other hand, by preventing C₂A from participating in effector interactions with the presynaptic membrane would result in a more severe disruption in evoked release (Fernandez-Chacon et al., 2001; Paddock et al., 2008; Paddock et al., 2011) than the D→N mutations.

Studies examining biochemical interactions between C₂A domains and negatively charged phospholipids *in vitro* may not fully reflect interactions *in vivo* due to the necessarily simplified environment of the *in vitro* assays. For instance, the positive charge of the Ca²⁺ bound to C₂A helps attract and bind negatively-charged liposomes *in vitro*. D→N mutations in isolated C₂A domains inhibit this lipid binding despite charge neutralization (Fernandez-Chacon et al., 2002; Robinson et al., 2002). But only 1 or 2 of the 5 negatively-charged aspartates are mutated in the D→N mutations tested. Thus, this partial charge neutralization may be insufficient to actively attract negatively-charged liposomes *in vitro*. Yet *in vivo*, active attraction by bound Ca²⁺ may not be necessary to permit near normal membrane interactions mediated by the remaining arginine and hydrophobic residues due to the

coordinated action of the SNARE-associated C₂B domain to pivot the C₂A pocket onto the presynaptic membrane. Additional interactions not modeled above are undoubtedly also involved.

By inhibiting Ca²⁺ binding yet maintaining the negative charge of the pocket, the syt^{A-D2E} mutation would interrupt *all* Ca²⁺-dependent interactions mediated by C₂A; the effect would not be limited to the membrane interactions discussed in our model above. Indeed, since the syt^{A-D2E} mutation results in an 80% decrease of synchronous release while the C₂A positively-charged or hydrophobic mutations inhibit only 50% (Fernandez-Chacon et al., 2001; Paddock et al., 2008; Paddock et al., 2011), the impact of Ca²⁺ binding to C₂A clearly influences *more* than just these interactions with the membrane. Thus, C₂A likely participates in additional electrostatic interactions upon Ca²⁺ binding that play a role in triggering synchronous release, perhaps with SNARE complexes or other effector molecules. Regardless of which C₂A interactions trigger fusion, the finding that C₂A D→N mutations support efficient synaptic transmission while our C₂A D→E mutation inhibits transmission by 80% demonstrates the central importance of the change in electrostatic potential of C₂A for triggering fusion.

In summary, our current findings show severe disruption of synchronous synaptic transmission *in vivo* caused by inhibiting Ca²⁺-binding by the C₂A domain *without* removal of the negative charge of the pocket. These results demonstrate that this negative charge in C₂A is a critical component of the electrostatic inhibition that prevents synaptic vesicle fusion. Thus, the essential function of Ca²⁺ binding to the C₂A domain of synaptotagmin is to neutralize this charge and, along with C₂B, to initiate the electrostatic switch mechanism that triggers vesicle fusion.

Acknowledgments

The authors thank Drs. Gary Pickard and Mike Tamkun for fruitful discussions and Dr. Deborah M. Garrity for comments on this manuscript. E.R.C. is an Investigator of the Howard Hughes Medical Institute. This work was supported by grants from the National Institutes of Health (NER:NS-045865, ERC:MN-61876), the National Science Foundation (NER:IOS-9982862 and -1025966), the Microscope Imaging Network and the College Research Council of Colorado State University.

References

- Bai J, Wang P, Chapman ER. C2A activates a cryptic Ca²⁺-triggered membrane penetration activity within the C2B domain of synaptotagmin I. *Proc Natl Acad Sci U S A*. 2002; 99:1665–1670. [PubMed: 11805296]
- Bhalla A, Chicka MC, Tucker WC, Chapman ER. Ca(2+)-synaptotagmin directly regulates t-SNARE function during reconstituted membrane fusion. *Nat Struct Mol Biol*. 2006; 13:323–330. [PubMed: 16565726]
- Brand A, Perrimon N. Targeted gene expression as a means of altering cell fates and generating dominant phenotypes. *Development*. 1993; 118:401–415. [PubMed: 8223268]
- Broadie K, Bellen HJ, DiAntonio A, Littleton JT, Schwarz TL. Absence of synaptotagmin disrupts excitation-secretion coupling during synaptic transmission. *Proc Natl Acad Sci U S A*. 1994; 91:10727–10731. [PubMed: 7938019]
- Brose N, Petrenko AG, Südhof TC, Jahn R. Synaptotagmin: a calcium sensor on the synaptic vesicle surface. *Science*. 1992; 256:1021–1025. [PubMed: 1589771]
- Chae YK, Abildgaard F, Chapman ER, Markley JL. Lipid binding ridge on loops 2 and 3 of the C2A domain of synaptotagmin I as revealed by NMR spectroscopy. *J Biol Chem*. 1998; 273:25659–25663. [PubMed: 9748232]
- Chapman ER, Davis AF. Direct interaction of a Ca²⁺-binding loop of synaptotagmin with lipid bilayers. *J Biol Chem*. 1998; 273:13995–14001. [PubMed: 9593749]

- Chapman ER, Hanson PI, An S, Jahn R. Ca²⁺ regulates the interaction between synaptotagmin and syntaxin 1. *J Biol Chem*. 1995; 270:23667–23671. [PubMed: 7559535]
- Cho W, Stahelin RV. Membrane binding and subcellular targeting of C2 domains. *Biochim Biophys Acta*. 2006; 1761:838–849. [PubMed: 16945584]
- Creighton, TE. *Proteins: Structure and Molecular Properties*. W. H. Freeman & Co; NY: 1994.
- Dai H, Shen N, Arac D, Rizo J. A quaternary SNARE-synaptotagmin-Ca²⁺-phospholipid complex in neurotransmitter release. *J Mol Biol*. 2007; 367:848–863. [PubMed: 17320903]
- Davis AF, Bai J, Fasshauer D, Wolowick MJ, Lewis JL, Chapman ER. Kinetics of synaptotagmin responses to Ca²⁺ and assembly with the core SNARE complex onto membranes. *Neuron*. 1999; 24:363–376. [PubMed: 10571230]
- Davletov B, Perisic O, Williams RL. Calcium-dependent membrane penetration is a hallmark of the C2 domain of cytosolic phospholipase A2 whereas the C2A domain of synaptotagmin binds membranes electrostatically. *J Biol Chem*. 1998; 273:19093–19096. [PubMed: 9668093]
- DiAntonio A, Parfitt KD, Schwarz TL. Synaptic transmission persists in *synaptotagmin* mutants of *Drosophila*. *Cell*. 1993; 73:1281–1290. [PubMed: 8100740]
- Dodge FAJ, Rahamimoff R. Co-operative action of calcium ions in transmitter release at the neuromuscular junction. *J Physiol (Lond)*. 1967; 193:419–432. [PubMed: 6065887]
- Elferink LA, Peterson MR, Scheller RH. A role for synaptotagmin (p65) in regulated exocytosis. *Cell*. 1993; 72:153–159. [PubMed: 8422678]
- Fernandez I, Arac D, Ubach J, Gerber SH, Shin O, Gao Y, Anderson RG, Südhof TC, Rizo J. Three-dimensional structure of the synaptotagmin I C₂B-domain: Synaptotagmin I as a phospholipid binding machine. *Neuron*. 2001; 32:1057–1069. [PubMed: 11754837]
- Fernandez-Chacon R, Königstorfer A, Gerber SH, Garcia J, Matos MF, Stevens CF, Brose N, Rizo J, Rosenmund C, Südhof TC. Synaptotagmin I functions as a calcium regulator of release probability. *Nature*. 2001; 410:41–49. [PubMed: 11242035]
- Fernandez-Chacon R, Shin O, Königstorfer A, Matos MF, Meyer AC, Garcia J, Gerber SH, Rizo J, Südhof TC, Rosenmund C. Structure/function analysis of Ca²⁺ binding to the C2A domain of synaptotagmin I. *J Neurosci*. 2002; 22:8438–8446. [PubMed: 12351718]
- Fuson KL, Montes M, Robert JJ, Sutton RB. Structure of human synaptotagmin I C2AB in the absence of Ca²⁺ reveals a novel domain association. *Biochemistry*. 2007; 46:13041–13048. [PubMed: 17956130]
- Herrick DZ, Sterbling S, Rasch KA, Hinderliter A, Cafiso DS. Position of synaptotagmin I at the membrane interface: cooperative interactions of tandem C2 domains. *Biochemistry*. 2006; 45:9668–9674. [PubMed: 16893168]
- Hui E, Johnson CP, Yao J, Dunning FM, Chapman ER. Synaptotagmin-mediated bending of the target membrane is a critical step in Ca(2+)-regulated fusion. *Cell*. 2009; 138:709–721. [PubMed: 19703397]
- Loewen CA, Mackler JM, Reist NE. *Drosophila synaptotagmin I* null mutants survive to early adulthood. *Genesis*. 2001; 31:30–36. [PubMed: 11668675]
- Loewen CA, Royer SM, Reist NE. *Drosophila synaptotagmin I* null mutants show severe alterations in vesicle populations but calcium-binding motif mutants do not. *J Comp Neurol*. 2006a; 496:1–12. [PubMed: 16528727]
- Loewen CA, Lee SM, Shin YK, Reist NE. C2B polylysine motif of synaptotagmin facilitates a Ca²⁺-independent stage of synaptic vesicle priming in vivo. *Molec Biol Cell*. 2006b; 17:5211–5226. [PubMed: 16987956]
- Mace KE, Biela LM, Sares AG, Reist NE. Synaptotagmin I stabilizes synaptic vesicles via its C2A polylysine motif. *Genesis: J Genetics Devmt*. 2009; 47:337–345.
- Mackler JM, Reist NE. Mutations in the second C₂ domain of synaptotagmin disrupt synaptic transmission at *Drosophila* neuromuscular junctions. *J Comp Neurol*. 2001; 436:4–16. [PubMed: 11413542]
- Mackler JM, Drummond JA, Loewen CA, Robinson IM, Reist NE. The C(2)B Ca(2+)-binding motif of synaptotagmin is required for synaptic transmission in vivo. *Nature*. 2002; 418:340–344. [PubMed: 12110842]

- Martens S, Kozlov MM, McMahon HT. How synaptotagmin promotes membrane fusion. *Science*. 2007; 316:1205–1208. [PubMed: 17478680]
- Morimoto T, Popov S, Buckley KM, Poo MM. Calcium-dependent transmitter secretion from fibroblasts: modulation by synaptotagmin I. *Neuron*. 1995; 15:689–696. [PubMed: 7546747]
- Murray D, Honig B. Electrostatic control of the membrane targeting of C2 domains. *Mol Cell*. 2002; 9:145–154. [PubMed: 11804593]
- Nalefski EA, Falke JJ. The C2 domain calcium-binding motif: structural and functional diversity. *Protein Sci*. 1996; 5:2375–2390. [PubMed: 8976547]
- Okamoto T, Tamura T, Suzuki K, Kidokoro Y. External Ca²⁺ dependency of synaptic transmission in drosophila synaptotagmin I mutants. *J Neurophysiol*. 2005; 94:1574–1586. [PubMed: 16061495]
- Paddock BE, Striegel AR, Hui E, Chapman ER, Reist NE. Ca²⁺-dependent, phospholipid-binding residues of synaptotagmin are critical for excitation-secretion coupling in vivo. *J Neurosci*. 2008; 28:7458–7466. [PubMed: 18650324]
- Paddock BE, Wang Z, Biela LM, Chen K, Getzy MD, Striegel A, Richmond JE, Chapman ER, Featherstone DE, Reist NE. Membrane penetration by synaptotagmin is required for coupling calcium binding to vesicle fusion in vivo. *J Neurosci*. 2011; 31:2248–2257. [PubMed: 21307261]
- Pang ZP, Shin OH, Meyer AC, Rosenmund C, Südhof TC. A gain-of-function mutation in synaptotagmin-1 reveals a critical role of Ca²⁺-dependent soluble N-ethylmaleimide-sensitive factor attachment protein receptor complex binding in synaptic exocytosis. *J Neurosci*. 2006; 26:12556–12565. [PubMed: 17135417]
- Reist NE, Buchanan J, Li J, DiAntonio A, Buxton EM, Schwarz TL. Morphologically docked synaptic vesicles are reduced in *synaptotagmin* mutants of *Drosophila*. *J Neurosci*. 1998; 18:7662–7673. [PubMed: 9742137]
- Rickman C, Archer DA, Meunier FA, Craxton M, Fukuda M, Burgoyne RD, Davletov B. Synaptotagmin interaction with the syntaxin/SNAP-25 dimer is mediated by an evolutionarily conserved motif and is sensitive to inositol hexakisphosphate. *J Biol Chem*. 2004; 279:12574–12579. [PubMed: 14709554]
- Robinson IM, Ranjan R, Schwarz TL. Synaptotagmins I and IV promote transmitter release independently of Ca(2+) binding in the C(2)A domain. *Nature*. 2002; 418:336–340. [PubMed: 12110845]
- Schiavo G, Stenbeck G, Rothman J, Sollner T. Binding of the synaptic vesicle v-SNARE, synaptotagmin, to the plasma membrane t-SNARE, SNAP-25, can explain docked vesicles at neurotoxin-treated synapses [see comments]. *Proc Natl Acad Sci U S A*. 1997; 94:997–1001. [PubMed: 9023371]
- Shao X, Davletov BA, Sutton RB, Südhof TC, Rizo J. Bipartite Ca²⁺-binding motif in C₂ domains of synaptotagmin and protein kinase C. *Science*. 1996; 273:248–251. [PubMed: 8662510]
- Shin OH, Xu J, Rizo J, Südhof TC. Differential but convergent functions of Ca²⁺ binding to synaptotagmin-1 C2 domains mediate neurotransmitter release. *Proc Natl Acad Sci U S A*. 2009; 106:16469–16474. [PubMed: 19805322]
- Stevens CF, Sullivan JM. The synaptotagmin C2A domain is part of the calcium sensor controlling fast synaptic transmission. *Neuron*. 2003; 39:299–308. [PubMed: 12873386]
- Stewart BA, Mohtashami M, Trimble WS, Boulianne GL. SNARE proteins contribute to calcium cooperativity of synaptic transmission. *Proc Natl Acad Sci U S A*. 2000; 97:13955–13960. [PubMed: 11095753]
- Sutton RB, Davletov BA, Berghuis AM, Südhof TC, Sprang SR. Structure of the first C2 domain of synaptotagmin I: a novel Ca²⁺/phospholipid-binding fold. *Cell*. 1995; 80:929–938. [PubMed: 7697723]
- Tamura T, Hou J, Reist NE, Kidokoro Y. Nerve-evoked synchronous release and high K⁺-induced quantal events are regulated separately by synaptotagmin I at *Drosophila* neuromuscular junctions. *J Neurophysiol*. 2007; 97:540–549. [PubMed: 17079341]
- Ubach J, Zhang X, Shao X, Südhof TC, Rizo J. Ca²⁺ binding to synaptotagmin: how many Ca²⁺ ions bind to the tip of a C2-domain? *EMBO*. 1998; 17:3921–3930.

- Wang P, Wang CT, Bai J, Jackson MB, Chapman ER. Mutations in the effector binding loops in the C2A and C2B domains of synaptotagmin I disrupt exocytosis in a nonadditive manner. *J Biol Chem*. 2003; 278:47030–47037. [PubMed: 12963743]
- Yao KM, White K. Neural specificity of elav expression: defining a Drosophila promoter for directing expression to the nervous system. *J Neurochem*. 1994; 63:41–51. [PubMed: 8207445]
- Yoshihara M, Littleton JT. Synaptotagmin I functions as a calcium sensor to synchronize neurotransmitter release. *Neuron*. 2002; 36:897–908. [PubMed: 12467593]
- Yoshihara M, Guan Z, Littleton JT. Differential regulation of synchronous versus asynchronous neurotransmitter release by the C2 domains of synaptotagmin I. *Proc Natl Acad Sci U S A*. 2010; 107:14869–14874. [PubMed: 20679236]
- Zhang X, Kim-Miller MJ, Fukuda M, Kowalchuk JA, Martin TF. Ca²⁺-dependent synaptotagmin binding to SNAP-25 is essential for Ca²⁺-triggered exocytosis. *Neuron*. 2002; 34:599–611. [PubMed: 12062043]

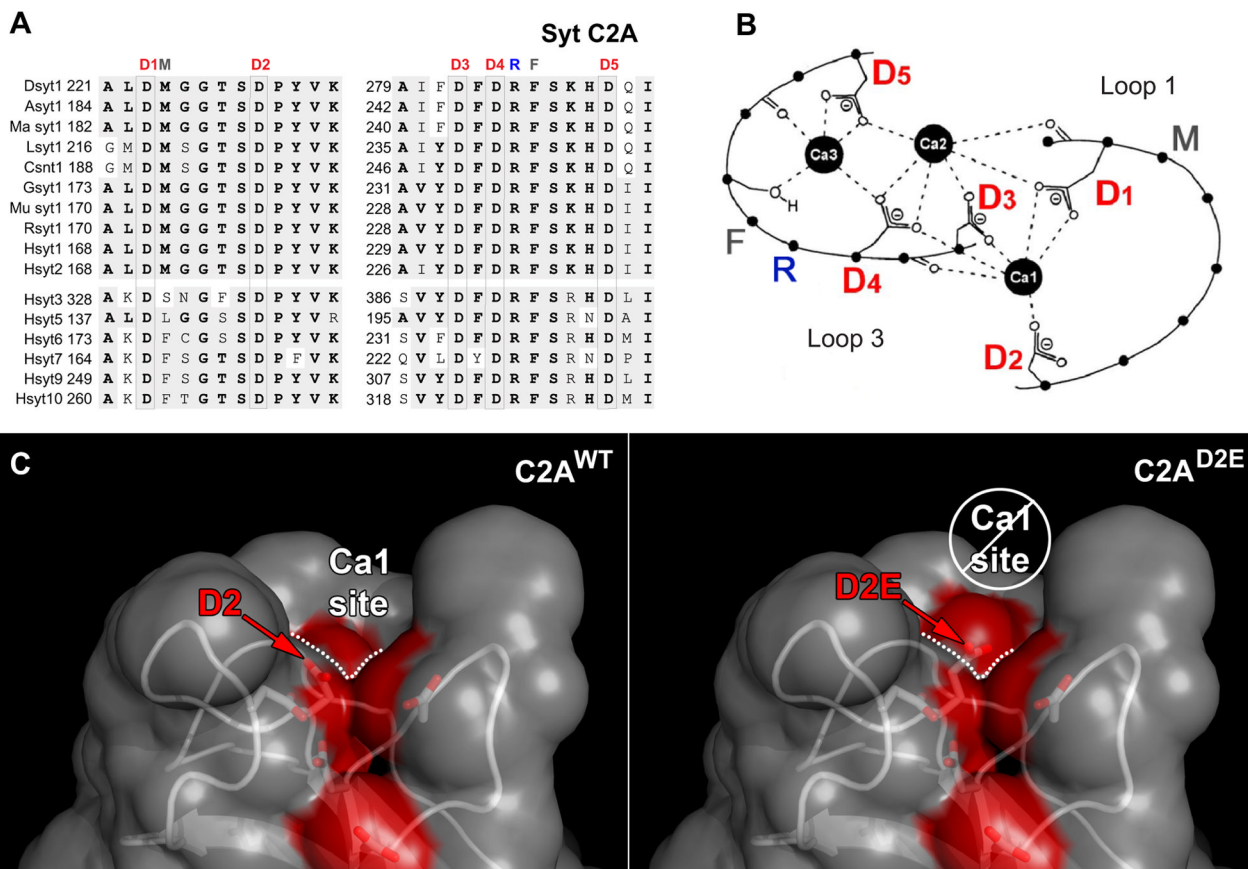


Figure 1.

The C₂A domain of synaptotagmin 1 has five highly conserved aspartate residues that coordinate Ca²⁺. **A**) Alignment of C₂A from Ca²⁺-binding synaptotagmin isoforms: synaptotagmin 1 from *Drosophila* (Dsyt1), bee (Asyt1), *Manduca* (Ma syt1), squid (Lsyt1), *C. elegans* (Csnt1), chicken (Gsyt1), mouse (Mu syt1), rat (Rsyt1) and human synaptotagmins 1–3, 5–7, 9 and 10 (Hsyts). Conserved residues are shown in grey and identical residues are in bold. The five conserved aspartate residues that coordinate the binding of Ca²⁺ ions are boxed and labeled as D1–D5. The conserved residues that mediate Ca²⁺-dependent interactions with negatively-charged membranes are also indicated by M, R, F. **B**) Schematic representation of loops 1 and 3 that form the Ca²⁺-binding pocket of the C₂A domain. Adapted from Fernandez et al. (Fernandez et al., 2001) to highlight the aspartates which coordinate Ca²⁺ (D1–5) as well as the residues that interact with membranes (M, R, F). **C**) Molecular model of the C₂A Ca²⁺-binding pocket illustrating the potential effect of the C₂A^{D2E} mutation. Coloring the oxygen atoms of the aspartate residues that coordinate Ca²⁺ by element revealed the negatively-charged Ca²⁺-binding sites on the solvent accessible surface (red). In rat syt 1, asp178 (D2, left panel) participates in the coordination of the first Ca²⁺ (Ca1 site indicated by dotted line, see also panel B). Using the mutagenesis function in PyMol, we modeled the consequences of altering asp178 to a glutamate (D2E, right panel). We predicted that the bulging out of the solvent accessible surface (enlarged red bulge above white dotted line, right panel) could prevent Ca²⁺ binding to the Ca1 site.

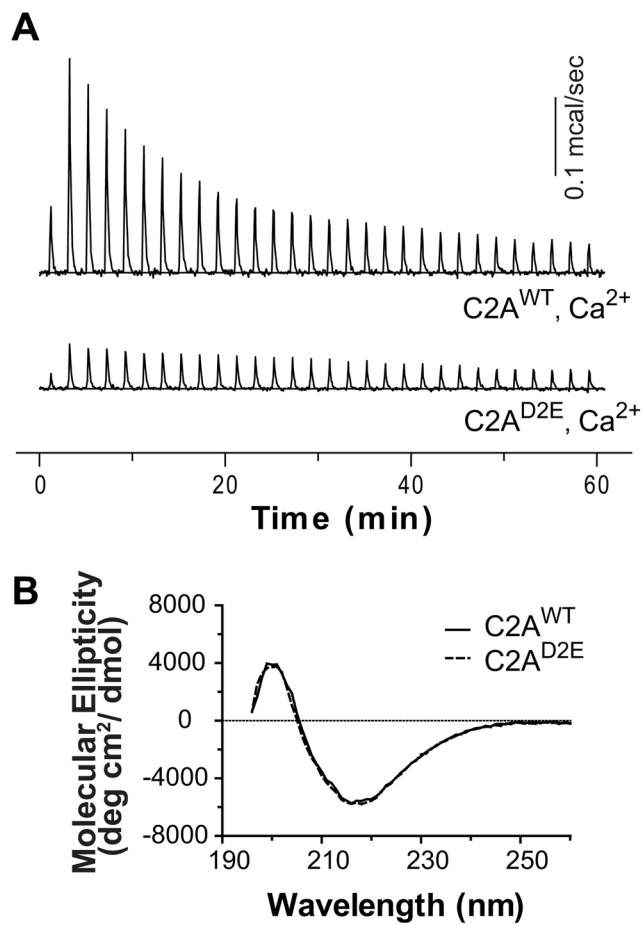


Figure 2. The C₂A^{D2E} mutation inhibits Ca²⁺ binding by C₂A without disrupting protein folding. **A)** ITC analysis of Ca²⁺ binding to the isolated C₂A domain of WT and mutant *Drosophila* synaptotagmin 1; a representative Ca²⁺ titration is shown (n = 3). C₂A^{WT} bound three calcium ions (see Table 1). The heat of binding of Ca²⁺ by C₂A^{D2E} was so small that the data could not be accurately fit. **B)** C₂A^{D2E} is correctly folded. The CD spectra of the mutant domain (C₂A^{D2E}) was identical to wild type (C₂A^{WT}).

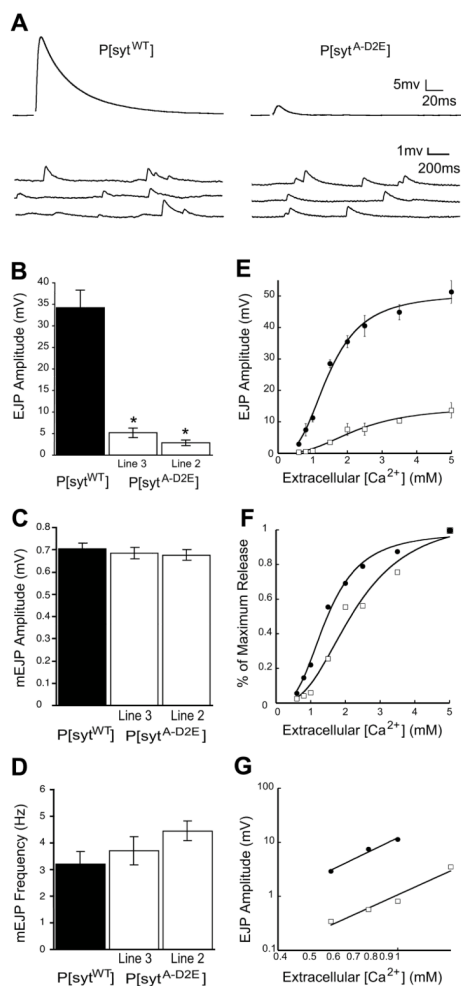


Figure 3.

Synchronous evoked release is severely impaired in C2A Ca^{2+} -binding mutants, but spontaneous release remains unchanged. **A)** Representative traces of EJPs and mEJPs recorded in saline containing 1.5 mM $[\text{Ca}^{2+}]$. **B)** Mean EJP amplitude was markedly decreased in $P[\text{syt}^{A-D2E}]$ mutants compared to $P[\text{syt}^{WT}]$ controls (mean \pm s.e.m., * $p < 0.001$, one way ANOVA). Neither mEJP amplitude (**C**, mean \pm s.e.m., $p > 0.7$, one way ANOVA) nor frequency (**D**, mean \pm s.e.m., $p > 0.15$, one way ANOVA) vary significantly between $P[\text{syt}^{A-D2E}]$ mutants compared to $P[\text{syt}^{WT}]$ controls. **E)** EJP amplitude vs. $[\text{Ca}^{2+}]$ fit with the Hill equation. Error bars, where visible, are s.e.m. For all panels, black circles indicate $P[\text{syt}^{WT}]$, white squares indicate $P[\text{syt}^{A-D2E}]$. **F)** Ca^{2+} dose response data normalized to the maximal response in each line to illustrate the decrease in apparent Ca^{2+} affinity in the $P[\text{syt}^{A-D2E}]$ mutant. **G)** EJP amplitudes within the non-saturating range of Ca^{2+} on a double-log plot demonstrate that the Ca^{2+} cooperativity of release is not changed in the $P[\text{syt}^{A-D2E}]$ mutants. A linear regression line was used to determine the slope.

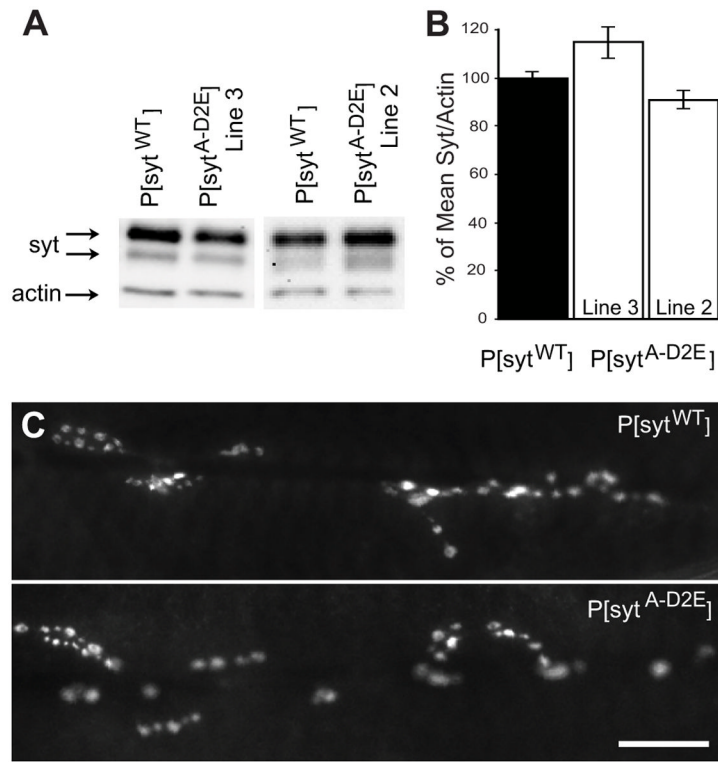


Figure 4. Synaptotagmin expression is similar in $P[syt^{A-D2E}]$ mutants compared to $P[syt^{WT}]$ controls. **A)** Representative Western blots of the central nervous system of third instar larvae probed with anti-synaptotagmin and anti-actin antibodies. **B)** Synaptotagmin/actin ratio normalized to the mean ratio of the transgenic control, $P[syt^{WT}]$. There was no significant difference between genotypes (mean \pm s.e.m., $p > 0.3$, one way ANOVA; $P[syt^{WT}]$ n=15, $P[syt^{A-D2E}]$ line #3 n=6, line #2 n=7). **C)** Synaptotagmin is properly localized to the larval neuromuscular junction in both mutant and control transgenic synaptotagmin lines. Scale 20 μm .

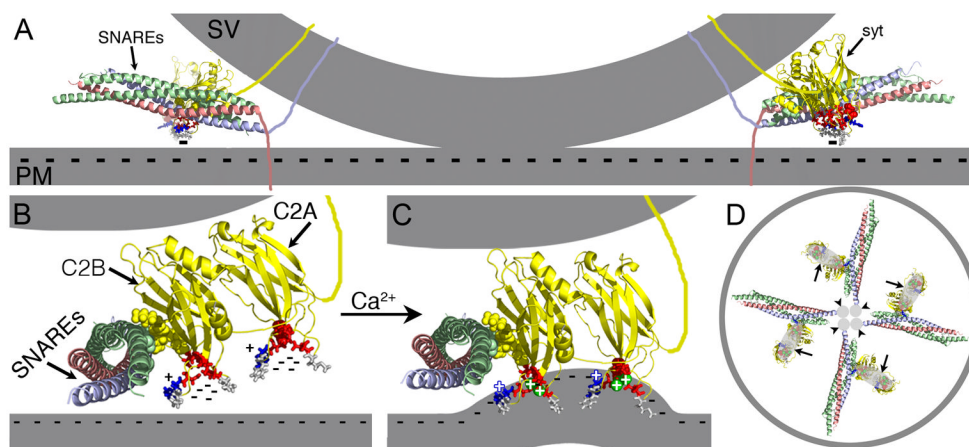


Figure 5.

Ca^{2+} binding by C2A is an essential component of the electrostatic switch. The crystal structure of the core complex [PDB file 1SFC, containing syntaxin (red), SNAP-25 (green), and VAMP/synaptobrevin (blue)], the NMR structures of the C2A (PDB file 1BYN) and C2B (PDB file 1K5W) domains of synaptotagmin (yellow), and Ca^{2+} (green spheres “+”) are shown to scale using PyMOL. The membranes, the transmembrane domains, and the link between C2A and C2B were added in Adobe Photoshop. **A)** Cross section of a docked vesicle showing two SNARE complexes (SNAREs) and their associated synaptotagmin molecules (syt). **B)** One syt/SNARE complex viewed from the site of vesicle/presynaptic membrane apposition. A Ca^{2+} -independent docking/priming interaction between the C2B polylysine motif (yellow, space-filled residues) and SNAP-25 [green, space-filled residues, (Rickman et al., 2004; Loewen et al., 2006b)] holds the C2B Ca^{2+} -binding site immediately adjacent to the presynaptic membrane with the C2A Ca^{2+} -binding site further removed. In the absence of Ca^{2+} , the conserved aspartate residues (red residues: syt^{C2A-D2}, space-filled; the rest as sticks) within the pockets create a high concentration of negative charge (cluster of “-”) resulting in electrostatic repulsion of the presynaptic membrane that prevents any membrane interactions by the tips of the C2 domains. **C)** Upon Ca^{2+} binding, the electrostatic repulsion of the pockets is neutralized thereby initiating the electrostatic switch: a strong attraction of the negatively-charged membrane by the bound Ca^{2+} (green spheres “+”) and the basic residues at the tips of Ca^{2+} -binding pockets (blue stick residues “+”). Insertion of the hydrophobic residues (grey stick residues) at the tips of the C2 domains into the core of the presynaptic membrane then triggers fusion by promoting a local Ca^{2+} -dependent positive curvature of the plasma membrane (Martens et al., 2007; Hui et al., 2009; Paddock et al., 2011). The C2 domain interactions with the membrane likely pull the synaptic vesicle (upper grey membrane) toward the presynaptic membrane (lower grey membrane). The Ca^{2+} -induced increase in positive charge at the end of the C2B domain also likely increases the strength of the electrostatic interaction between the C2B polylysine motif and the SNARE complex, resulting in simultaneous binding of the SNARE complex and the presynaptic membrane (Davis et al., 1999; Bhalla et al., 2006; Loewen et al., 2006a; Dai et al., 2007). **D)** Membrane penetration by multiple synaptotagmins (large grey ovals, arrows) would pull the plasma membrane toward the vesicle in a ring around the SNARE transmembrane domains (small grey circles, arrowheads) facilitating fusion.

Table 1Thermodynamic properties of calcium binding to C₂A^{WT} using ITC.

K_D (μM)	ΔH (cal/mol)	ΔS (cal/mol/K)	ΔG (kcal/mol)
K _{D1} = 20.7 ± 3.9	ΔH ₁ =1005 ± 72.3	ΔS ₁ = 24.9 ± 0.12	ΔG ₁ = -6.17
K _{D2} = 83.4 ± 19	ΔH ₂ = 407.5 ± 166	ΔS ₂ = 20.1 ± 0.35	ΔG ₂ = -5.38
K _{D3} = 766 ± 302	ΔH ₃ = 2406 ± 597	ΔS ₃ = 22.7 ± 1.3	ΔG ₃ = -4.13

Data represent mean ± SD, n = 3.